A R C H I V E S O F M E T A L L U R G Y A N D M A T E R I A L S
Volume 59 2014 Issue 4
DOI: 10.2478/amm-2014-0223

A. SZKLINIARZ*, L. BLACHA*, W. SZKLINIARZ*, J. ŁABAJ*

CHARACTERISTICS OF PLASTICITY OF HOT DEFORMED Cu-Ti ALLOYS

CHARAKTERYSTYKI PLASTYCZNOŚCI ODKSZTAŁCANYCH NA GORĄCO STOPÓW Cu-Ti

In the paper, results of a study on the effects of deformation conditions (temperature, strain and strain rate) on flow curves, maximum flow stress and corresponding deformation of Cu-Ti alloys with various Ti contents, subjected to hot deformation, are presented. Evaluation of formability of alloys was performed with the use of a Gleeble HDS-V40 thermal-mechanical simulator during uniaxial hot compression at 700 to 900°C, strain rate of 0.1 to 10.0 s^{-1} and strain of 0 to 1.2 (70%). It was found that within the analysed ranges of temperature, strain rate and strain, Cu-Ti alloys underwent uniform deformation without cracking. The largest deformation resistances were observed for the alloys with the highest Ti contents; their decrease was possible with the temperature raise and the strain rate reduction.

Keywords: copper-titanium alloy, hot compression test, plasticity, flow curves

W pracy przedstawiono wyniki badań wpływu warunków odkształcenia (temperatura, wielkość i prędkość odkształcenia) na przebieg krzywych płynięcia, wartość maksymalnego naprężenia uplastyczniającego i odpowiadającego mu odkształcenia odkształcanych plastycznie na gorąco stopów Cu-Ti o zróżnicowanej zawartości Ti. Ocenę podatności do kształtowania plastycznego stopów przeprowadzono na symulatorze cieplno-mechanicznym systemu Gleeble HDS-V40 w warunkach jednoosiowego ściskania na gorąco w zakresie temperatury od 700 do 900°C, prędkości odkształcenia od 0.1 do 10.0 s^{-1} i odkształcenia od 0 do 1.2 (70%). Stwierdzono, że w analizowanych przedziałach temperatury, prędkości i wielkości odkształcenia stopy Cu-Ti odkształcają się w sposób jednorodny bez udziału pękania. Wykazano, że największe opory kształtowania plastycznego towarzyszą stopom o najwyższej zawartości Ti, a ich zmniejszenie jest możliwe poprzez podwyższenie temperatury i obniżenie prędkości odkształcenia.

1. Introduction

A wide use of copper and its alloys results from their excellent electric and thermal conductivities as well as extremely high corrosion resistance, high strength and formability. Among manufactured copper alloys, precipitation-hardened beryllium bronzes (also called beryllium coppers) show the highest strength level. Moreover, they demonstrate good electrical conductivity, good formability during hot and cold working as well as a non-sparking quality [1].

Essential disadvantages of beryllium bronzes are high prices and toxic properties. Due to their toxicity, the use of beryllium bronzes has been forbidden for many years in Poland and EU countries as beryllium compounds are hazardous during melting and casting as well as bonding, welding, hot deformation, cutting and grinding [1, 2].

For many years, worldwide studies have been focused on discovering cheaper and non-toxic substitutes for Cu-Be alloys. Currently, the best substitutes for beryllium bronzes seem to be precipitation-hardened Cu-Ti alloys containing up to 5% mass titanium (6% at.) [1, 3-15]. Cu-Ti alloys, called titanium bronzes or copper titanium, show mechanical and electrical properties comparable to those of beryllium bronzes and they also have the non-sparking quality [1, 6, 8, 9, 11, 12, 14]. Due to this, they can be applied for production of high-strength springs as well as elements resistant to corrosion and abrasion, as electronic components, electrical connections, contacts, relays, electrical wires, gears and as components of equipment for anti-terrorist and mining rescue units.

Titanium bronzes are obtained in processes of melting in vacuum induction furnaces and casting to produce ingots [16]. Following homogenising annealing, the ingots are processed to yield semi-products and finished products during hot and cold working processes separated by intermediate annealing. Their final properties are obtained in processes of precipitation hardening, i.e. linked procedures of solution heat treatment and aging.

Properties of Cu-Ti alloys (titanium bronzes) result from the titanium content, the size of matrix (copper-titanium solid solution) grain, the overall deformation during cold working and morphologies of generated (during solution heat treatment and aging) dispersed precipitates of intermetallic phases formed between the alloy components [1, 5, 6, 8, 11, 13-15]. Size of grains of Cu-Ti semi-products and finished products

* SILESIAN UNIVERSITY OF TECHNOLOGY, FACULTY OF MATERIALS ENGINEERING AND METALLURGY, 8 KRASINSKIEGO STR., 40-019 KATOWICE, POLAND

are formed during hot working and intermediate annealing which precedes cold working [3, 4, 7, 9,]. Development of the backgrounds for the technology of hot working of Cu-Ti ingots needed plastometric investigations [17] to determine the best deformation conditions (temperature, strain rate and strain) to avoid cracking and to produce the required size of matrix grain.

The aim of the paper was assessment of technological plasticity of Cu-Ti alloys with various Ti contents, subjected to hot deformation at various temperatures and strain rates.

2. Experimental procedure

The study materials were three Cu-Ti alloys containing, respectively, 1.0, 2.0 and 3.0% mass Ti. The alloys were obtained in the Seco/Warwick VIM 20-50 vacuum induction furnace [18-21], in a magnesite crucible. The charge materials were oxygen-free copper MOOB of high purity and a master alloy: Cu-30%mass Ti. The alloys were casted into graphite moulds to produce ingots of 40 mm in diameter and the length of 350 mm. Following casting, the ingots were subjected to homogenising annealing at 850°C for 24 hours which was ended by cooling with the furnace. The next step was hot rolling at 950÷850°C using a shape rolling mill to yield rods of 12 mm in diameter. The rods were used for preparing samples for the plastometric tests.

Evaluation of formability of the investigated alloys was performed with the use of a Gleeble HDS-V40 thermal-mechanical simulator during uniaxial hot compression. The process of hot compression is illustrated in Fig. 1. According to it, the rolling samples (10 mm in diameter, 18 mm high) were subjected to resistance heating at 3°C/s under the vacuum to reach 950°C. After 5-minute heating at that temperature, the samples were cooled at 10°C/s to the set deformation temperature and heated at that temperature for 1 minute, followed by compression until the relative strain of 70% was obtained (corresponding to the true deformation of 1.2) at the assumed strain rate of 0.1, 1.0 or 10.0 s^{-1}. The stress changes versus true deformation were recorded. When the set deformation was achieved, the samples were cooled in water. To reduce friction, graphite foil was placed between gripping heads and the sample.

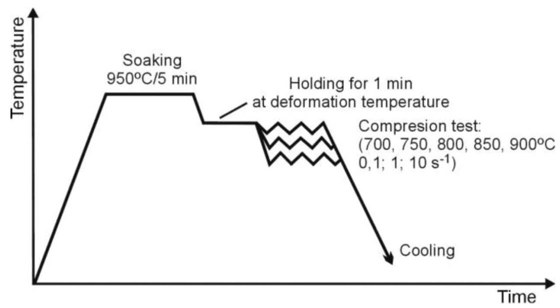

Fig. 1. Flow diagram of compression tests studied Cu-Ti alloys

Preparation of materials for microstructure investigations involved cutting with the use of a circular cutting-off machine and an electrical discharge machine, wet grinding, mechanical polishing on oxide and diamond pastes, etching in the mixture of 25 g ammonium persulfate and 100 ml H_2O as well as the 15% HNO_3 solution. The microstructure investigations were conducted with a Nikon Epiphot 200 microscope; the cross-section perpendicular to the axis of the ingot or compressed sample was analysed.

The x-ray phase analysis of investigated alloys was conducted with the use of a Jeol JDX-7S diffractometer with a copper anode (powered by the 20 mA, 40 kV current) and a graphite monochromator. For the investigations of cross-section perpendicular to the axis, samples obtained from the ingot were used.

3. Results and discussion

The Cu-Ti ingots (melted in a vacuum induction furnace and casted into a graphite mould) show a characteristic dendritic microstructure with many precipitates (spheroid to elongated in shape) that are evenly arranged in the interdendritic spaces (Fig. 2a). The x-ray analysis of the alloy phase compositions showed that the two phase microstructure consisted of the α phase, which is the Cu-Ti solid solution, and

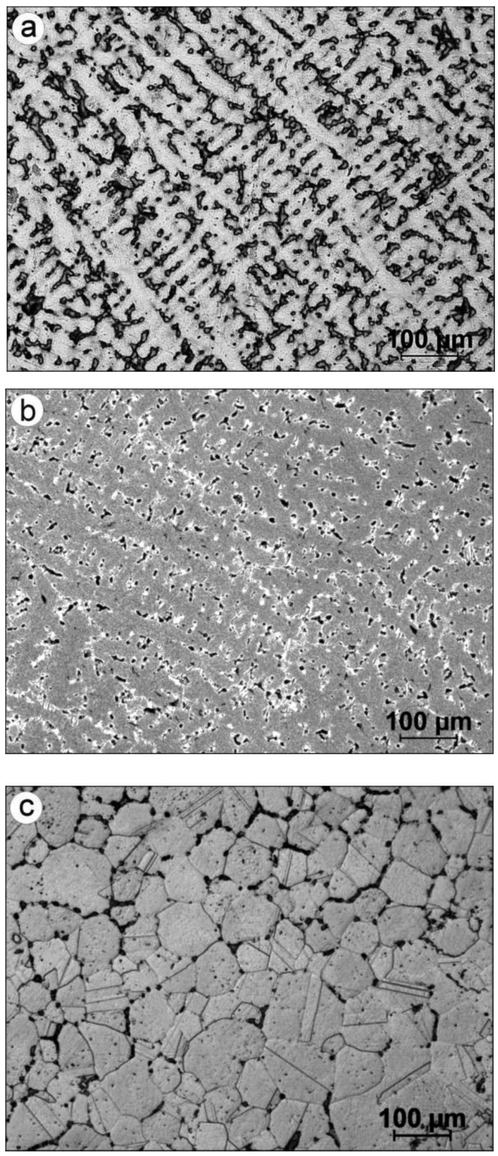

Fig. 2. Microstructure of Cu-3Ti alloy after casting (a), homogenizing (b) and hot rolling (c)

the titanium-rich intermetallic Cu_3Ti phase (Fig. 3). With increased titanium contents in Cu-Ti alloys, the relative volume of the intermetallic Cu_3Ti phase, present in the interdendritic spaces, successively increases (Fig. 4).

The dendritic microstructure, typical of post-casting alloys (Fig. 2a), partly loses its characteristics following homogenising annealing (Fig. 2b); however, it still contains the intermetallic Cu_3Ti phase precipitates of markedly smaller sizes and relative volumes.

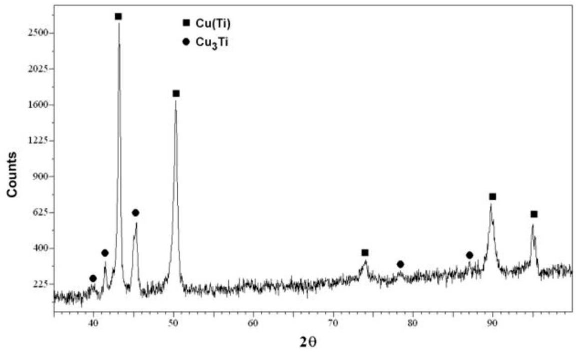

Fig. 3. The XRD diffraction spectra of Cu-3Ti alloy after casting

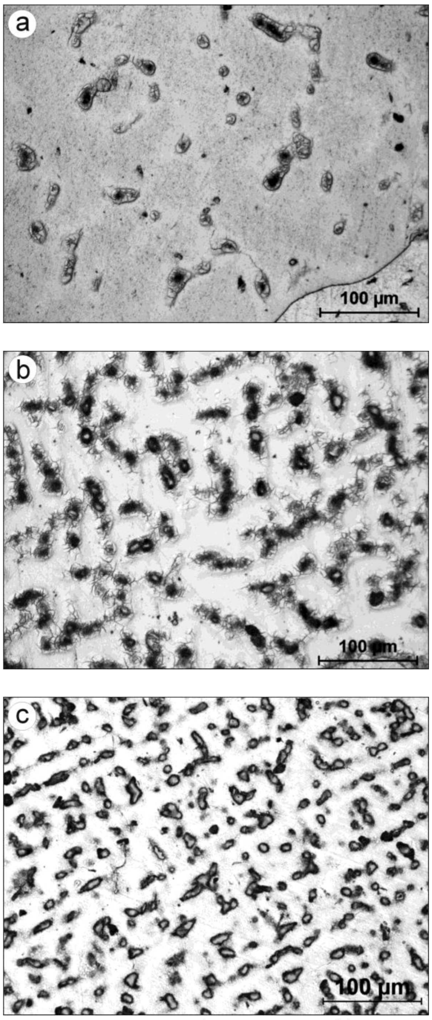

Fig. 4. Microstructure of the alloy Cu-1Ti (a), Cu-2Ti (b) and Cu-3Ti (c) after casting

After hot rolling, the investigated Cu-Ti alloys show a uniform, equiaxial grain microstructure of moderate grain size with large precipitates of the intermetallic Cu_3Ti phase at the grain boundaries and remarkably smaller ones inside (Fig. 2c).

The investigations of formability of Cu-Ti alloys with various titanium contents (1.0, 2.0 and 3.0% mass), conducted during uniaxial compression, confirmed that within the whole temperature range (700÷900°C) and at the strain rates of 0.1, 1.0 and 10.0 s^{-1}, the alloys underwent uniform deformation without cracking. This is evidenced by no buckling effect of the shape as well as the appearance of side and flat surfaces of the samples following compression (Fig. 5).

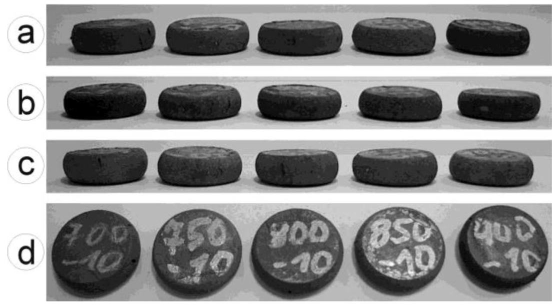

Fig. 5. Appearance of Cu-3Ti alloy specimens after compression at temperature in the range 700÷900°C up to a strain of 1.2 (70%) with strain rate of 0.1 (a), 1.0 (b) and 10.0 s^{-1} (c)

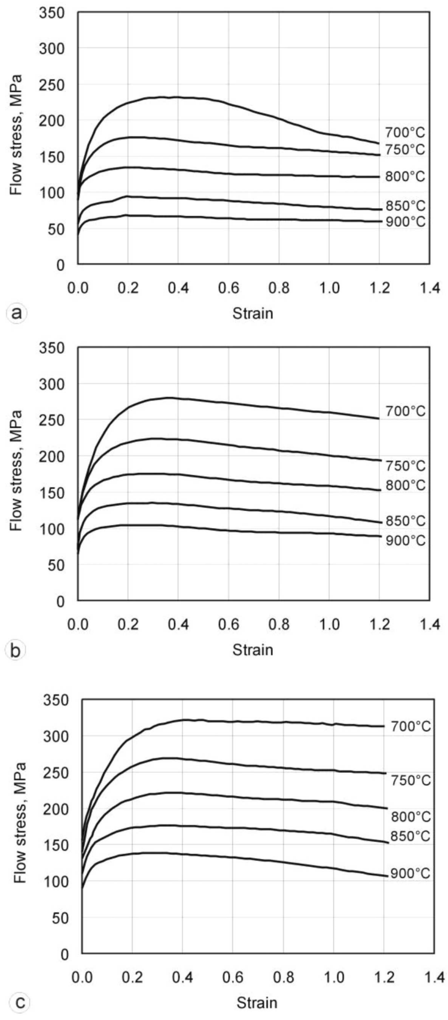

Fig. 6. Flow curves of Cu-3Ti alloy deformed at different temperature with strain rate of 0.1 (a), 1.0 (b) and 10.0 s^{-1} (c)

As shown in Fig. 6, for the Cu-3Ti alloy with the highest Ti content and the lowest deformability expected, within the investigated deformation temperature range (700÷900°C), all flow curves demonstrate a characteristic initial increase in flow stress to reach its maximum, followed by monotonic decrease. This may indicate the presence of structure rebuilding processes, e.g. dynamic recrystallisation, in the material subjected to hot deformation. Similar flow curves were observed for the alloys with lower Ti contents.

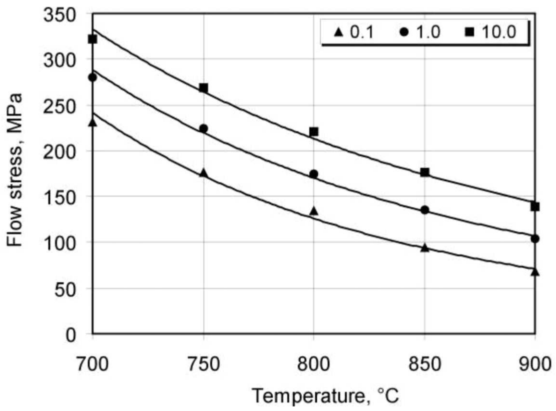

Fig. 7. Change of peak flow stress of Cu-3Ti alloy with varying deformation temperature and strain rate

Fig. 7, which illustrates the effects of temperature on maximum values of flow stress (σ_m) for various strain rates of the same alloy, shows a strong reduction of maximum flow stress for specific strain rates when the temperature is raised and the strain rate is decreased. Moreover, strong effects of higher Ti contents in Cu-Ti alloys on the increase of peak flow stress were observed, particularly for a lower deformation temperature (Fig. 8, Table 1).

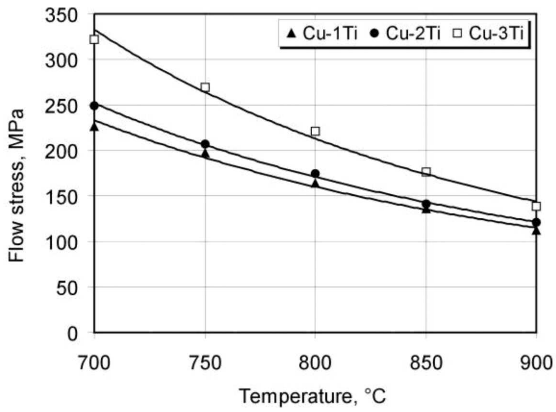

Fig. 8. Change of peak flow stress of Cu-Ti alloys deformed at different temperature with strain rate of 10.0 s^{-1}

The effect of strain rate on the maximum flow stress is more distinct if presented in the semi-logarithmic system (Fig. 9) which shows that for a specific temperature, the increase of strain rate strongly enhances the flow stress, particularly when the rate is 10.0 s^{-1}. Presentation of the Fig. 9 data in the double-logarithmic system (Fig. 10) confirms a relationship between the peak flow stress (σ_m) and the strain rate ($\dot{\varepsilon}$) for a specific temperature:

$$\sigma_m = K \cdot \dot{\varepsilon}^m \tag{1}$$

where: K is a constant and m is the strain rate sensitivity index.

TABLE 1

Peak flow stress σ_m and strain corresponding to the peak flow stress ε_m hot deformed Cu-Ti alloys

Temperature, °C	**700**		**750**		**800**		**850**		**900**	
Strain rate, s^{-1}	σ_m MPa	ε_m	σ_m MPa	ε_m	σ_m MPa	ε_m	σ_m MPa	ε_m	σ_m MPa	ε_m
Cu-1Ti										
0.1	149	0.47	117	0.43	92	0.43	71	0.38	55	0.28
1.0	192	1.04	154	0.79	122	0.59	101	0.48	81	0.39
10.0	226	1.01	197	1.04	164	1.02	136	1.00	112	1.00
Cu-2Ti										
0.1	184	0.37	132	0.27	102	0.24	76	0.24	56	0.23
1.0	216	0.41	171	0.39	138	0.35	108	0.35	84	0.34
10.0	249	0.46	207	0.45	175	0.42	141	0.40	121	0.39
Cu-3Ti										
0.1	231	0.34	176	0.22	134	0.20	94	0.19	68	0.18
1.0	280	0.33	224	0.30	175	0.28	135	0.25	104	0.23
10.0	322	0.40	269	0.36	221	0.37	176	0.31	139	0.28

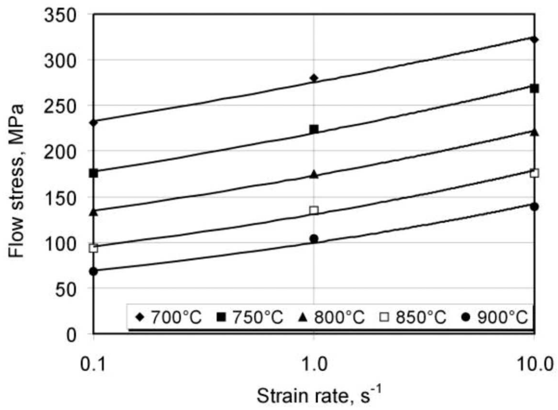

Fig. 9. Change of peak flow stress of Cu-3Ti alloy with varying strain rate and deformation temperature

The m values for the investigated alloys with various Ti contents, calculated based on the slopes in e.g. Fig. 10, fall within 0.07÷0.18. They show a linearly increasing relationship with temperature (Fig. 11) and decrease with higher Ti contents in the alloy. A specific range of the m changes clearly demonstrates that Cu-Ti alloys, within the analysed temperature and strain rate ranges, do not show superplastic deformability.

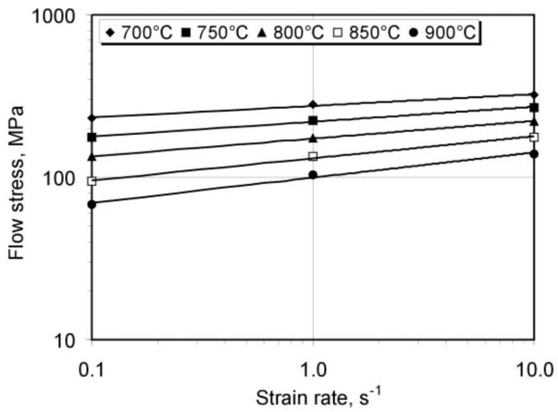

Fig. 10. Change of peak flow stress of Cu-3Ti alloy with varying strain rate and deformation temperature as log-log plots

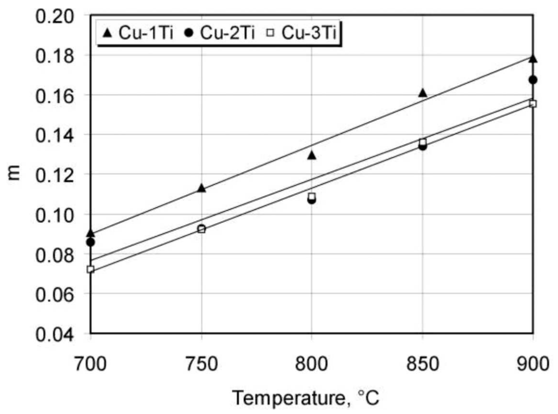

Fig. 11. Change of strain rate sensitivity of Cu-Ti alloys with varying deformation temperature

Temperature and the strain rate also affect the strain corresponding to the maximum flow stress (ε_m) (Fig. 12, Table 1). Higher temperatures and smaller strain rates result in lower strain. When it is reached, further deformation depends on processes of dynamic recrystallisation in the material subjected to deformation.

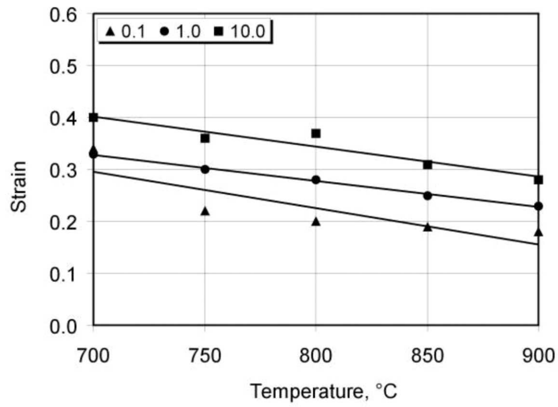

Fig. 12. Change of strain corresponding to the peak flow stress of Cu-3Ti alloy with varying deformation temperature and strain rate

In the alloy with the highest Ti content and the lowest deformability property, processes of microstructure rebuilding (which lead to its softening) start when the true deformation level of 0.2÷0.4 is reached. To initiate similar processes in the alloy with the lowest Ti content, true deformation of at least 1.0 is required (Fig. 13, Table 1). Increased Ti contents in Cu-Ti alloys result in markedly reduced strain corresponding to the maximum flow stress: not only for the strain rate of 10.0 s^{-1} (Fig. 13) but also for the other two analysed strain rates (Table 1).

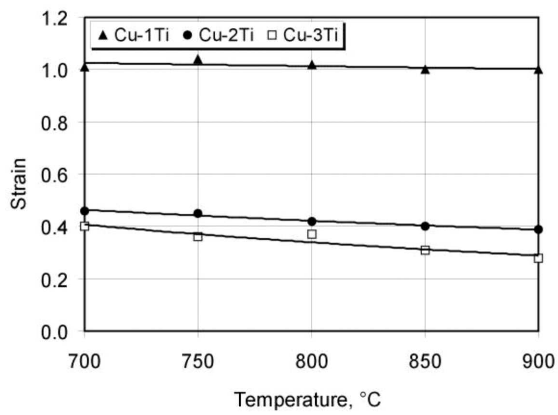

Fig. 13. Change of strain corresponding to the peak flow stress of Cu-Ti alloys deformed at different temperature with strain rate of 10.0 s^{-1}

4. Conclusions

Cu-Ti alloys with Ti contents of 1.0÷3.0% at., obtained during melting in a vacuum induction furnace and casting into graphite moulds, show a two phase microstructure consisting of the α phase (the Cu-Ti solid solution) and the Ti-rich intermetallic Cu_3Ti phase whose relative volume increases with a higher Ti content in the alloy.

The investigations of formability of these alloys showed that within the 700÷900°C range and at the strain rate of 0.1÷10.0 s^{-1} as well as with the true deformation of 0÷1.2, their deformation is uniform without cracking.

The flow curves, illustrating stress changes versus true deformation for Cu-Ti alloys subjected to hot compression, show a characteristic initial increase of flow stress to reach its maximum, followed by monotonic decrease resulting from dynamic recrystallisation.

The value of true deformation which triggers dynamic recrystallisation in hot-deformed Cu-Ti alloys falls within 0.2÷1.0. It decreases with the increased Ti content in the alloy, higher temperature and smaller strain rate values.

Hot deformation of Cu-Ti alloys is accompanied by moderate deformation resistances; their measure is the value of maximum flow stress. The highest deformation resistances are observed for the alloy with the highest Ti content. Reduction of deformation resistances is possible with the temperature raise and the strain rate reduction.

In the case of Cu-Ti alloys, there is a statistically significant relationship between the maximum flow stress and the strain rate, which is observed when the strain rate sensitivity index is 0.07÷0.18. The index value shows that these alloys, within the analysed temperature and strain rate ranges, do not demonstrate a superplastic flow quality.

Acknowledgements

The study was conducted under the Research Project No. R 15 004 02, financed by the Ministry of Science and Higher Education – Poland.

REFERENCES

[1] Z. Rdzawski, Miedź stopowa, Wydawnictwo Politechniki Śląskiej, Gliwice (2009).
[2] M. Madej, Bezpieczeństwo pracy nauka i praktyka **5**, 26-28 (1999).
[3] D.E. Laughlin, J. Cahn, Acta Metall. Mater. **23**, 329-339 (1975).
[4] S. Nagarjuna, M. Srinivas, K. Balasubramanian, D.D. Sarma, Acta Metall. Mater. **44**, 2285-2293 (1996).
[5] S. Nagarjuna, K. Balasubramanian, D.D. Sarma, Mat. Sci. Eng. A **225**, 118-124 (1997).
[6] S. Nagarjuna, M. Srinivas, K. Balasubramanian, D.D. Sarma, Int. J. Fatigue **19**, 51-57 (1997).
[7] A.A. Hameda, L. Błaż, Mat. Sci. Eng. A **254**, 83-89 (1998).
[8] S. Nagarjuna, M. Srinivas, K. Balasubramanian, D.D. Sarma, Mat. Sci. Eng. A **259**, 34-42 (1999).
[9] S. Nagarjuna, K. Balasubramanian, D.D. Sarma, J. Mater. Sci. **34**, 2929-2942 (1999).
[10] H. Okamoto, J. Phase Equilib. **23** (3), 549-550 (2002).
[11] S. Nagarjuna, M. Srinivas, Mat. Sci. Eng. A **335**, 89-93 (2002).
[12] S. Suzuki, K. Hirabayashi, H. Shibata, K. Mimura, M. Isshiki, Y. Waseda, Scripta Mater. **48**, 431-435 (2003).
[13] W.A. Sofa, D.E. Laughlin, Prog. Mater. Sci. **49**, 347-366 (2004).
[14] S. Nagarjuna, M. Srinivas, Mat. Sci. Eng. A **406**, 186-194 (2005).
[15] L. Blacha, G. Siwiec, A. Kościelna, A. Dudzik-Truś, Inżynieria Materiałowa **6** (172), 520-524 (2009).
[16] A. Szkliniarz, W. Szkliniarz, Solid State Phenom. **176**, 139-148 (2011).
[17] A. Szkliniarz, Solid State Phenom. **176**, 149-156 (2011).
[18] J. Łabaj, B. Oleksiak, G. Siwiec, Metalurgija **50** (4), 265-268 (2011).
[19] J. Łabaj, Archives of Metallurgy and Materials **57** (1), 166-172 (2012).
[20] G. Siwiec, Archives of Metallurgy and Materials **58** (4), 1155-1160 (2013).
[21] L. Blacha, J. Mizera, P. Folęga, Metalurgija **53** (1), 51-54 (2014).

Received: 20 January 2014.